

Lasing on higher-azimuthal-order modes in vertical cavity surface emitting lasers at room temperature

C.-J. Cheng · Y.Y. Lin · C.-Y. Chen · T.-D. Lee ·
R.-K. Lee

Received: 23 February 2009 / Revised version: 20 August 2009 / Published online: 3 October 2009
© Springer-Verlag 2009

Abstract We report a direct method to observe higher-azimuthal-order whispering-gallery-like modes in vertical cavity surface emitting lasers (VCSELs) at room temperature. Instead of introducing any defect mode, we show that suppression of lower-order cavity modes can be achieved by destroying vertical reflectors with a surface micro-structure. Perfect higher-order modes with an azimuthal number as large as 41 are observed in experiments through collecting near-field radiation patterns, as well as in numerical simulations.

PACS 42.55.Px · 42.55.Sa · 05.45.Mt

1 Introduction

Whispering-gallery (WG) modes are almost grazing incidence patterns confined by total internal reflection at an interface [1, 2]. With advantages of an ultra-small mode volume and a strong confinement, WG modes have attracted lots of attention in photonics, quantum electrodynamics, and telecommunications due to their potential applications to enhance spontaneous emission and make threshold-less lasing. In the last decade WG modes have been experimen-

tally demonstrated with semiconductor micro-cavities, including micro-disk [3, 4], micro-ring [5], micro-sphere [6], and other novel micro-resonators [7]. For a two-dimensional (2D) structure, in the beginning a waveguide is used to provide the confinement of light in the vertical direction for WG modes. With optical output vertically emitted from the surface, vertical cavity surface emitting lasers (VCSELs) are a natural choice for lasers with transverse behavior of a vertical emission and a WG-like mode [8], even though strictly speaking the propagation vectors of the light in these modes are nearly perpendicular to the plane of the active layer.

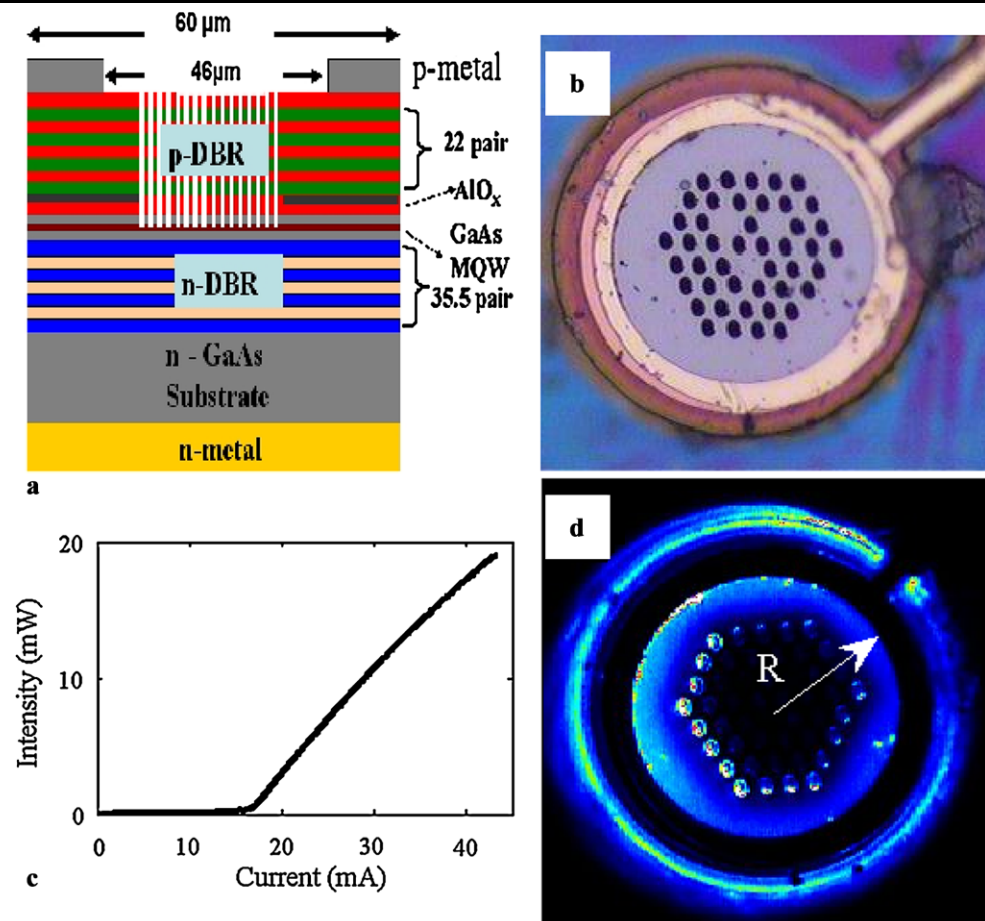
In recent years, with the advance of new fabrication technologies, it has become more and more feasible to actually utilize one- or higher-dimensional periodic dielectric structures (or especially the photonic band gap crystals) to modify the resonance modes in semiconductor lasers [9]. Combined with the band-gap effect and micro-cavities, an ultra-high quality factor for a single-defect semiconductor laser formed by a 2D photonic crystal was reported [10]. Applications based on WG modes, which act as filters, delay lines, couplers, and sensors, cover a broad areas from optical communications, information processing, to biophotonics [11]. Consequentially, the control of WG modes in optical resonators plays a crucial role for every specific application. Given a refractive index in 2D disks or rings, the order of modes in the azimuthal direction is proportional to the radius of the disks or rings and inversely proportional to the lasing wavelength. Following this guideline, the WG modes supported in photonic crystal defect cavities are typically lowest-order modes due to the fact that the defect geometry is usually on the same order of magnitude as the lasing wavelength. To excite WG modes with a larger azimuthal number, micro-disks or micro-rings with a broad area have been introduced [12], which also act as an interesting platform for studying optical pattern

C.-J. Cheng · Y.Y. Lin · C.-Y. Chen · R.-K. Lee (✉)
Institute of Photonics Technologies, National Tsing-Hua
University, Hsinchu 300, Taiwan
e-mail: rkleee@ee.nthu.edu.tw

T.-D. Lee
Graduate School of Optoelectronics, National Yunlin University
of Science and Technology, Yunlin 640, Taiwan

T.-D. Lee
Industrial Technology Research Institute, Hsinchu 310, Taiwan

Fig. 1 (a) The schematic diagram, (b) corresponding SEM image, and (c) L–I curve for our VCSEL with the surface micro-structure. (d) The near-field collected spontaneous emission pattern below the threshold current, with $R = 30 \mu\text{m}$



formation in mesoscopic systems [13, 14]. Although very high-azimuthal-order modes in optical cavities have been reported in the literature [14–16], it is well known that spatial mode structures in these broad-area VCSELs suffer problems of instabilities and nonlinearities.

Due to the competitions between different modes, a cryogenic system is needed to suppress unwanted cavity modes in a large-area VCSEL, in order to compensate the temperature-dependent shift in the gain peak [13, 17]. In this work, we propose another simple but robust method to directly excite required transverse optical patterns by a 2D micro-structure on a VCSEL surface [10, 12, 18]. Instead of forming a defect cavity, we show that it is possible to use the surface structure as a deterioration mechanism for the desired lasing characteristics. As most of the vertical emission windows in the central region are destroyed by the surface micro-structure, we report direct observations of an ultra-high-order WG-like mode lasing, with an azimuthal number as large as 41. All demonstrations of WG-like mode lasings are directly collected by their near-field radiation intensities at room temperature, and verified by a 2D mode solver in simulations. The experimental and numerical investigations in this work provide a new direction for applying higher-

azimuthal-order WG modes in areas as diverse as quantum optics, communications, and chaotic dynamics.

2 Characteristics of the micro-surfaced VCSEL

Figure 1a and b show the schematic diagram and the corresponding scanning electron microscope (SEM) image of the surface micro-structured VCSEL used in our experiments, respectively. The epitaxial layers of the VCSEL are grown by metal organic chemical vapor deposition (MOCVD) on an n^+ -GaAs substrate, with a graded-index separate confinement heterostructure (GRINSCH) active region formed by undoped triple-GaAs–AlGaAs quantum wells placed in a $1-\lambda$ cavity. The upper and bottom distributed Bragg reflectors (DBRs) in the vertical cavity consist of 22 and 35.5 pairs of $\text{Al}_{0.1}\text{Ga}_{0.9}\text{As}/\text{Al}_{0.9}\text{Ga}_{0.1}\text{As}$ layers, respectively. We introduce an oxide aperture to reduce the lateral optical loss and leakage current. Then, reactive ion etch (RIE) is performed to define mesas, where the $\text{Al}_{0.98}\text{Ga}_{0.02}\text{As}$ layer within the $\text{Al}_{0.9}\text{Ga}_{0.1}\text{As}$ confinement layers is selectively oxidized to AlO_x . The thickness of the oxide layer is about 300 \AA (within a quarter- λ layer, and $\lambda = 850 \text{ nm}$). The p-contact ring with an inner diameter of $46 \mu\text{m}$ and a width

of $7\ \mu\text{m}$ is formed on the top of the p-contact layer, i.e. $R = 30\ \mu\text{m}$. The n-contact is formed at the bottom of the n-GaAs substrate. Detailed device parameters and lasing characteristics can be found in our previous publication on a similar VCSEL device but with a different surface micro-structure [19]. The micro-structured surface pattern is defined by the focused ion beam, with the depth of the holes estimated to reach the active layer. A hexagonal lattice pattern is fabricated within the p-contact ring to introduce a surface micro-structure. The lattice constant and diameter for this hexagonal micro-structured VCSEL are 5 and $3\ \mu\text{m}$, respectively. Three defects in the micro-structure are introduced to suppress the lasing of lower-order cavity modes.

Figure 1c shows the L–I curve, light versus current, of the VCSEL with a surface micro-structure on it. The threshold current for lasing operation is about $17\ \text{mA}$. The increment of the threshold current is expected, since there is no lasing on the defect modes. Then, we show the measured near-field electromagnetic intensity distribution on the surface of the aperture by a charge-coupled-device (CCD) camera through a standard microscope with a $\times 100$ lens. When the VCSEL is operated below the threshold condition, for example in Fig. 1d, it can be seen clearly that the spontaneous emission pattern just reflects the lateral cavity defined by the native oxide layer in the VCSEL and the micro-surface structure within. As expected, in this case no significant emissions come from the center of the designed surface micro-structure. The radiation patterns are shown almost in the outside region, with some leaky radiations along the mesas. In our design of the surface micro-structure, the inner defects are fabricated with an offset from the center. In such a case, in contrast to the expected lasing mode in the inner region, only the outer ring has the chance to lase due to the symmetry-broken geometry in our cavity.

3 Near-field images of higher-order mode lasing

Again, as shown in Fig. 2a and b for the injection currents of $11\ \text{mA}$ and $13\ \text{mA}$, still far below the threshold condi-

tion, we can see clearly that the emission patterns are located along the outer region of the designed micro-structure, resulting in the form of a ring. It clearly demonstrates the accumulation of radiation fields in the outside ring as the injection current increases. Above the threshold current, the VCSEL begins to lase. Owing to the destruction of the top DBR reflector induced by the surface micro-structure, lower-order cavity modes are totally suppressed and the surrounding WG modes have a chance to lase. In Fig. 3a and c, operated at $19\ \text{mA}$ and $20.5\ \text{mA}$, perfect ultra-high-order WG-like grazing patterns confined by the total internal reflection with multiple lobes in the azimuthal direction are directly observed at room temperature. By counting the number of lobes, we report the recorded experimental demonstration of highest-order WG mode to the best of our knowledge, up to the azimuthal number of 41 . As is well known, there should be a trade-off between the threshold current and the excitation of higher-order modes. Here, the observations of higher-azimuthal-order WG-like modes are achieved at the scarification of increasing the threshold current.

To illustrate the experimental observation of a higher-azimuthal-order WG-like mode lasing in such a surface micro-structured VCSEL, we used a 2D mode solver based on the standard finite-element method for electromagnetic waves to calculate the corresponding eigenmodes of this laser cavity [20]. Here, due to the optical field confined by two DBR mirrors with the oxide layer of thickness of about $300\ \text{\AA}$ in the vertical direction, in this case we can safely reduce the three-dimensional (3D) model to an effective 2D model by estimating the effective index. The lateral geometry defined by the native oxide layer is drawn according to the observed spontaneous emission pattern below the threshold current, as shown in Fig. 1d. Then, micro-structures are embedded within the real lattice geometries. The effective refractive indices are assumed to be 1 in the holes and 3.49 in the surrounding SiO_2 oxide layer. In the numerical simulations, we calculate all possible eigenmodes and then select the most matching one for a comparison. The reason one can do this is due to the fact that these higher-order modes

Fig. 2 Near-field intensity distributions on the surface of the aperture of our micro-structured VCSEL below the threshold condition, at (a) 11-mA and (b) 13-mA injection currents, respectively

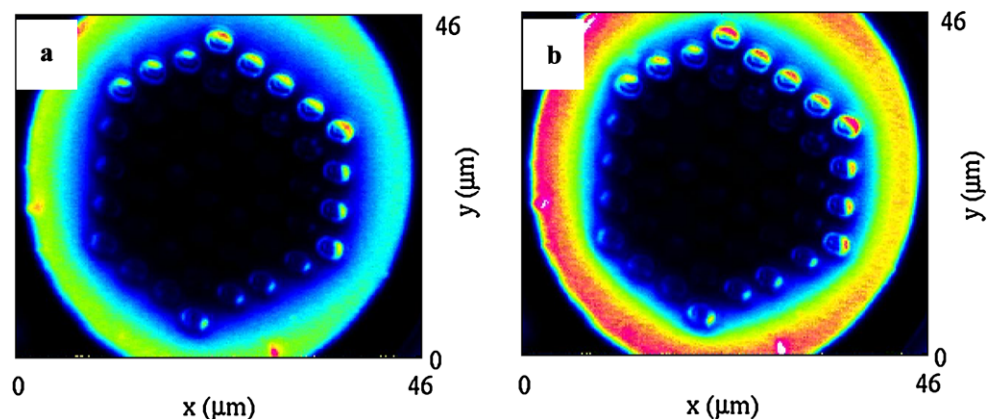
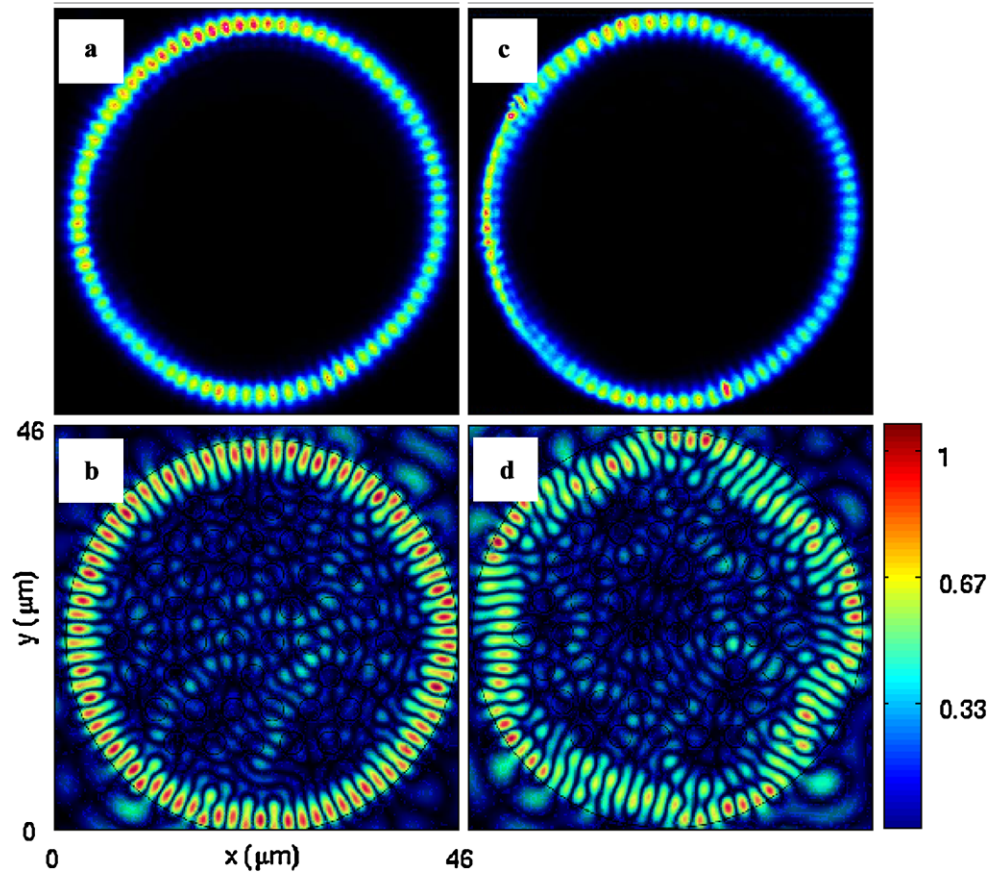


Fig. 3 Near-field intensity distributions on the surface of the aperture of our micro-structured VCSEL at different injection currents. Experimental data: (a) 19 mA and (c) 20.5 mA; and simulation results: (b) and (d) with the same number of lobes, 41, in the azimuthal direction. The intensity distributions are shown in an arbitrary unit



are nearly degenerate in such a broad-area VCSEL, with very close eigenwavelengths around the lasing wavelength at 850 nm. One of the calculated eigenmodes is shown in Fig. 3b. Compared to the experimental measurements in Fig. 3a and c, our numerical simulations show that the WG-like mode pattern existing in our cavity is not only with the same azimuthal number, 41, but also with a slightly asymmetric intensity distribution along the outer ring. From direct numerical simulations, the observed asymmetric intensity distributions in the azimuthal direction are believed to come from the inner micro-structure geometry, which overall is in the shape of a hexagon and breaks the rotational symmetry of the emission pattern. Moreover, one can see that the images are dark in the center for the experimental data, while some emissions are found in the numerical results. The discrepancy between experimental and numerical images may come from the 2D model we used. One possible solution is to perform a 3D simulation or to re-estimate the effective index, for the depth of our micro-structured surface pattern is too deep.

In Fig. 3d, we report another interesting quasi-WG mode supported in our designed surface micro-structure numerically. This quasi-WG mode also has the same number, 41, in the azimuthal direction, but with a chaotic field distribution. This chaotic behavior may be used to tailor the mode and the

resulting emission would be of great interest to researchers using ideas from quantum chaos to develop efficient and highly directional micro-lasers [19]. But, due to the competition with normal WG modes, which are more stable, the experimental observation for such an unusual mode at room temperature seems to be difficult.

4 Conclusion

In conclusion, with surface micro-structures and near-field technologies we investigate the formation of transverse optical patterns in GaAs-based VCSELs. A unique surface structure is designed to ruin the vertical reflector as well as to suppress the lasing characteristics for the lower-order cavity modes. At the expense of a higher threshold current, a native oxide laterally confined whispering-gallery mode in VCSELs can be directly observed at room temperature. Perfect WG-like modes up to the 41st order in the azimuthal direction are reported by collecting the near-field intensity on the surface of the aperture. The observed higher-azimuthal-order WG-like mode patterns are explained and identified by a direct numerical simulation. Through the help of surface micro-structures, especially with an offset from the center to break the geometric symmetry, the spatial patterns demonstrated in this work are more robust above threshold. The

experimental observations and the simulation results provide an alternative but easy approach to access WG modes in VCSELs at room temperature.

Acknowledgements The authors are indebted to H.P.D. Yang for providing the samples. This work is partly supported by the National Science Council of Taiwan with contracts NSC 95-2112-M-224-001, NSC 96-2112-M-224-001, NSC 95-2112-M-007-058-MY3, and NSC 95-2120-M-001-006.

References

1. R.K. Chang, A.J. Campillo (eds.), *Optical Processes in Microcavities* (World Scientific, Singapore, 1996) and references therein
2. A.B. Matsko, V.S. Ilchenko, IEEE J. Sel. Top. Quantum Electron. **12**, 3 (2006)
3. S.L. McCall, A.F.J. Levi, R.E. Slusher, S.J. Pearton, R.A. Logan, Appl. Phys. Lett. **60**, 289 (1992)
4. T.D. Lee, P.H. Cheng, J.S. Pan, R.S. Tsai, Y. Lai, K. Tai, Appl. Phys. Lett. **72**, 2223 (1998)
5. Y. Kawabe, Ch. Spiegelberg, A. Schulzgen, M.F. Nabor, B. Kippelen, E.A. Mash, P.M. Allemand, M. Kuwata-Gonokami, K. Takeda, N. Peyghambarian, Appl. Phys. Lett. **72**, 141 (1998)
6. V. Lefevre-Seguin, S. Haroche, Mater. Sci. Eng. B **48**, 53 (1997)
7. T.M. Benson, S.V. Boriskina, P. Sewell, A. Vukovic, S.C. Greedy, A.I. Nosich, in *Frontiers of Planar Lightwave Circuit Technology: Design, Simulation and Fabrication*, ed. by S. Janz, J. Ctyroky, S. Tanev (Springer, Berlin, 2005), pp. 39–70
8. H. Soda, K. Iga, C. Kitahara, Y. Suematsu, Jpn. J. Appl. Phys. **18**, 2329 (1979)
9. J.D. Joannopoulos, R.D. Meade, J.N. Winn, *Photonic Crystals: Molding the Flow of Light* (Princeton University Press, Princeton, 1995) and references therein
10. O. Painter, R.K. Lee, A. Scherer, A. Yariv, J.D. O'Brien, P.D. Dapkus, I. Kim, Science **284**, 1819 (1999)
11. K. Vahala (ed.), *Optical Microcavities* (World Scientific, Singapore, 2004)
12. T. Baba, IEEE J. Sel. Top. Quantum Electron. **3**, 808 (1997)
13. K.F. Huang, Y.F. Chen, H.C. Lai, Y.P. Lan, Phys. Rev. Lett. **89**, 224102 (2002)
14. T. Gensty, K. Becker, I. Fischer, W. Elsässer, C. Degen, P. Debernardi, G.P. Bava, Phys. Rev. Lett. **94**, 233901 (2005)
15. T. Ackemann, S. Barland, M. Cara, S. Balle, J.R. Tredicce, R. Jager, M. Grabherr, M. Miller, K.J. Ebeling, J. Opt. B: Quantum Semiclass. Opt. **2**, 406 (2000)
16. J. Scheuer, M. Orenstein, D. Arbel, J. Opt. Soc. Am. B **19**, 2384 (2002)
17. M. Schulz-Ruhtenberg, I.V. Babushkin, N.A. Loiko, T. Ackemann, K.F. Huang, Appl. Phys. B **81**, 945 (2005)
18. T.D. Lee, C.-Y. Chen, Y.Y. Lin, M.-C. Chou, T.-H. Wu, R.-K. Lee, Phys. Rev. Lett. **101**, 084101 (2008)
19. Y.Y. Lin, C.-Y. Chen, W. Chien, J.-S. Pan, T.-D. Lee, R.-K. Lee, Appl. Phys. Lett. **94**, 221112 (2009)
20. D.D. de Menezes, M. Jar e Silva, F.M. de Aguiara, Chaos **17**, 023116 (2007)